

INFLUENCE OF THE RATIO BETWEEN DILATANCY ANGLE AND INTERNAL FRICTION ANGLE ON STRESS DISTRIBUTION BEHIND A GRAVITY RETAINING WALL

Magdalena KOWALSKA *

* Dr.; Faculty of Civil Engineering, Department of Geotechnics and Roads, Silesian University of Technology, ul. Akademicka 5, 44-100 Gliwice, Poland
E-mail address: magdalena.kowalska@polsl.pl

Received: 10.08.2014; Revised: 21.10.2014; Accepted 16.01.2015

Abstract

The paper presents results of a numerical study of the influence of dilatancy angle on stress distribution behind a gravity retaining wall. The analysis has been conducted with the use of the finite element method. Elastic-perfectly plastic constitutive model with Coulomb-Mohr failure criterion was applied to simulate coarse soil behaviour. Twelve cases with different values of internal angle of friction φ' (30° , 36° or 42°) and the ratio α between the dilatancy angle ψ' and φ' (0, 1/3, 2/3 or 1) were considered. The analysis has revealed that the influence of the choice of dilatancy angle value is observed mainly at the lowest part of the retaining wall, where the pressure acting on the wall is the highest. The resultant maximum stress may be there even 30% higher when α changes from 1 to 0, which is probably the main reason of the observed lower bearing capacity or divergence of calculations in the cases when the difference between ψ' and φ' is greater than 20° .

Streszczenie

W pracy przedstawiono wyniki analizy numerycznej wpływu kąta dylatacji na rozkład naprężeń za ścianą oporową. Analiza ta została przeprowadzona przy użyciu metody elementów skończonych. Do opisu zachowania gruntu użyto modelu sprężysto-idealnie plastycznego z kryterium zniszczenia Coulomba-Mohra. Uwzględniono dwanaście przypadków z różnymi wartościami kąta tarcia wewnętrznego φ' (30° , 36° lub 42°) i stosunkiem α między wartościami kąta dylatacji ψ' i φ' (0, 1/3, 2/3 lub 1). Analiza wykazała, że wpływ wyboru wartości kąta dylatacji obserwowano głównie w najniższej części ściany oporowej, gdzie ciśnienie działające na ścianki jest najwyższe. Powstałe maksymalne naprężenie może być tam nawet o 30% wyższe gdy α zmienia się od 1 do 0, co jest prawdopodobnie głównym powodem obserwowanej niższej nośności lub rozbieżności obliczeń w przypadkach gdy różnica między ψ' i φ' jest większa niż 20° .

Keywords: Dilatancy angle; Internal angle of friction; Gravity retaining wall; Coulomb-Mohr model; Stress distribution; Numerical FEM analysis.

1. INTRODUCTION

In the classical analytical methods used in the engineering design of retaining walls (e.g. based on Coulomb [1] or Rankine's [2] theory) it is assumed that soil is a rigid – ideally plastic material, which means that there is no strain observed until the failure criterion is achieved. Only three cases are taken into account: the minimal *active* pressure (plastic equilibrium

in expansion) – when soil moves or rotates outwards from the wall, the *at-rest* pressure (elastic equilibrium), when there is no lateral displacement and the *passive* pressure (plastic equilibrium in contraction), when the wall moves towards the soil. Distribution of stress along the wall height is believed to be triangular or, when surcharge load is present, trapezoidal. To mobilize the maximum or the minimum value of stress the observed lateral displacement

of the wall should achieve some critical value, which in a real case may not occur [3, 4].

A numerical analysis with the use of finite element method (FEM) and even very simple elasto-plastic constitutive model with Coulomb-Mohr failure criterion (CM) has an advantage over the analytical calculations, as it makes it possible to consider gradual yielding of soil. As a consequence, it becomes possible to estimate not only the state of stress acting on the wall's face in the three cases mentioned above (active, at-rest or passive), but to solve a complex, true, soil – structure interaction problem in terms of evaluation of stresses and strains in the whole mass of soil surrounding the retaining wall and at each stage of loading. The results of such a study may be next compared with the *in situ* measurements of displacements.

Obviously the quality, reliability and accuracy of the outcome depend greatly on the selection of the constitutive model and estimation of their parameters' values.

The proper definition of yielding in the CM model requires estimation of the effective values of internal angle of friction φ' and cohesion c' , which describe the yield surface $F(p', q, \theta) = 0$, and the effective value of dilatancy angle ψ' which defines the potential surface $G(p', q, \theta) = 0$ and determines whether the plastic flow rule is associated ($\psi' = \varphi'$) or non-associated ($\psi' \neq \varphi'$). The two first parameters can be usually assessed based on the results of basic field or laboratory tests. The dilatancy angle value, however, is most often taken *a priori*, without any oriented research, even though just like all the other parameters of the CM model, it has a physical meaning and so could be estimated experimentally as the ratio between a plastic volumetric strain increment $\delta\varepsilon_{vol}^p$ and a plastic shear strain increment $\delta\varepsilon_s^p$. The observed dilatancy angle varies from about 0° to less than φ' . For sands and gravels with internal angle of friction $\varphi' > 30^\circ$ the dilatancy angle usually equals $\psi' = \varphi' - 30^\circ$.

In solving back-analysis problems, e.g. as a part of a procedure of global calibration of a numerical model, in which CM model is used, the dilatancy angle is quite often treated as a variable in order to fit the field measurements to the FEM results. It becomes then a coefficient of regression, without any physical meaning.

It is worth noting here that the dilatancy angle is absent, when the pressure exerted on a retaining wall is calculated analytically according to Coulomb's or Rankine's theory – it means thus that $\psi' = \varphi'$ is assumed.

2. PURPOSE OF THE RESEARCH AND ITS BACKGROUND

The purpose of the research presented in this paper is determination of the influence of the ratio between the dilatancy angle and the internal angle of friction ($\alpha = \psi'/\varphi'$) on the theoretical distribution of stress behind a retaining wall with a surcharge load, when estimated with the use of a numerical FEM analysis. The results will be compared with the ones obtained on the basis of the Rankine's theory.

The numerical model of the gravity retaining wall chosen for these calculations is the same one, which was analysed and described by the Author in the conference paper [5], in which the influence of ψ' on bearing capacity and rotation of the wall was examined. It was there concluded that an increase of ψ' value results in decrease of rotation and increase of the allowable load. It was also revealed that if the difference between ψ' and φ' is greater than 20° convergence problems occur and it is then impossible to achieve failure of the structure numerically.

According to the Author's knowledge so far there are no publications about the impact of dilatancy angle on distribution of stress mobilized behind a retaining wall with the loaded backfill. Three publications, however, are worth mentioning:

- 1) according to Serrano et al. [6], who analysed theoretically the pressures acting on retaining walls with the use of Hoek-Brown law, the lateral stress should increase with the increase of dilatancy angle;
- 2) mobilization of active earth pressure analysed numerically in [7] proved that with $\psi' = 0^\circ$ (non-dilatant flow) an arching effect at deeper levels of backfill behind a wall moving horizontally outwards is observed, resulting in nonlinear distribution of stress, which increased with wall displacement;
- 3) the nonlinear distribution of lateral stress and its dependency on the mode of wall movement (translation, rotation about the wall's top or base) was also noticed by Potts and Fourie [3] (unfortunately with no information about the value of the dilatancy angle).

Table 1.
Values of parameters used in the analysis (γ' – unit weight, ν – Poisson ratio, c' – cohesion, E – Young modulus, K_0 – coefficient of earth pressure at rest)

	γ' kN/m ³	ν -	c' kPa	E MPa	φ' °	K_0 -	ψ' °
Soil	20	0.25	5	40	30	0.5	0 / 10 / 20 / 30
				170	36	0.41	0 / 12 / 24 / 36
				240	42	0.33	0 / 14 / 28 / 42
Retaining wall	25	0.2	-	29 000	-	-	-

3. NUMERICAL ANALYSIS

3.1. Model

The influence of dilatancy angle was analysed on an example of a concrete gravity retaining wall embedded in a dry non-cohesive soil. Plane strain mode was considered in the FEM code ZSoil 2012 Student v.12.19. The soil was modelled with the use of CM theory and the wall was described with a linear elastic constitutive model. Interface elements were inserted between the soil and the wall to achieve their independent displacements. The overall size of the model was 7.5 m (height) and 12.0 m (width). The shape and dimensions of the gravity wall, its loading and a fragment of the finite elements mesh are presented in Fig. 1, together with the definition of a resultant stress σ_{res} and its inclination δ . The surcharge load q was applied along the distance of 2.45 m, starting 5 cm from the wall.

Twelve combinations of different values of internal angle of friction φ' (30°, 36° and 42°) and dilatancy angle ψ' ($= 0^\circ$, $= 1/3 \varphi'$, $= 2/3 \varphi'$, $= \varphi'$) were considered. The parameter values applied to all the finite elements are listed in Table 1.

It was assumed that the different values of internal angles of friction correspond to three different soils, e.g. fine sand, coarse sand and gravel – hence the variation in the values of Young moduli, which were assumed accordingly based on PN-81/B-03020 [8]. The values of coefficient of earth pressure at rest K_0 were calculated based on the well-known formula by Yaky [9]:

$$K_0 = 1 - \sin \varphi' \quad (1)$$

The non-zero cohesion, which can be explained by interlocking of grains (see e.g. [10, 11]), was applied to avoid numerical problems at the model surface. The values of interface elements' parameters were assumed, in accordance to [12], dependent on their location. So, in the elements under the wall $\varphi'_{cont} = \varphi'$ was applied, in elements behind the wall

(surcharge side) it was: $\varphi'_{cont} = 2/3 \varphi'$ and in front of the wall: $\varphi'_{cont} = 1/2 \varphi'$. The dilatancy angle values of interface elements were applied just like in the soil model as a proportion of φ'_{cont} . The surcharge load was increased gradually in 5 kPa (or smaller) steps until divergence occurred.

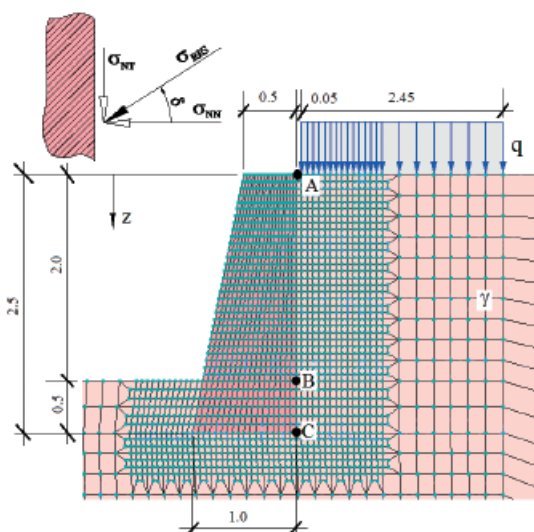


Figure 1. Shape and dimensions of the gravity wall (a fragment of FEM mesh) and definitions of resultant stress σ_{res} and inclination angle δ

3.2. Results

The resultant stress σ_{res} distributions for the cases where $\varphi' = 36^\circ$ and surcharge loads $q = 0$ kPa, 40 kPa, 80 kPa and 120 kPa are presented in Fig. 2. In case of $\varphi' = 30^\circ$ and $\varphi' = 42^\circ$ the surcharge loads of 0 kPa, 20 kPa, 40 kPa, 60 kPa and 0 kPa, 80 kPa, 160 kPa, 240 kPa were considered respectively (called further 0_SL , 2_SL , 4_SL and 6_SL), as it was established that the bearing capacities of the wall were about two times smaller when $\varphi' = 30^\circ$ and two times greater when $\varphi' = 42^\circ$. Because of the necessity of keeping the paper as concise as possible, only the results for the case of $\varphi' = 36^\circ$ are presented graphically.

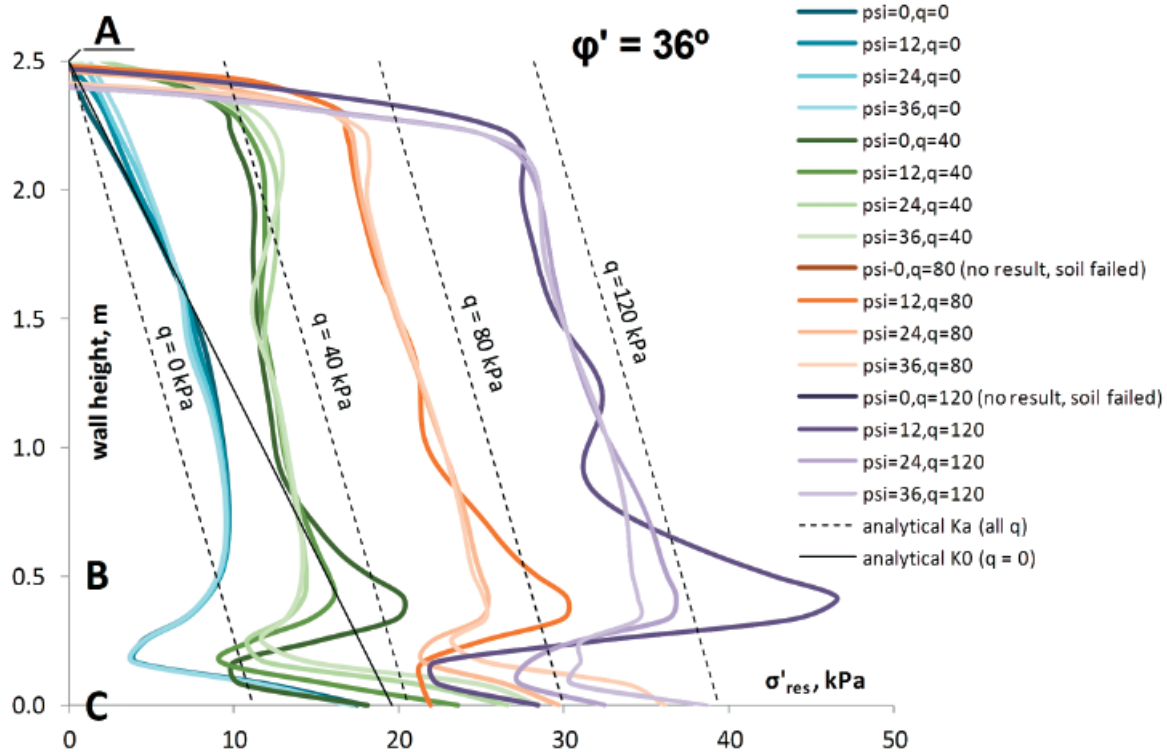


Figure 2. Resultant stress distributions along the segment A-C ($\varphi' = 36^\circ$)

The cross-section was drawn parallel to the wall through the centres of the first layer of finite elements simulating soil – at the distance of 2.5 cm from the wall. Similarly like in [3] and [7], the stress distribution is nonlinear. Due to arching caused by the existence of interface elements and the fact that the surcharge load is not applied directly above the elements, which are considered, the stress at the top of the wall is close to 0 kPa, no matter which surcharge load is applied. For 0_SL the graph along the AB segment is parabolic and for 2_SL – saddle-like. Only in the cases 4_SL and 6_SL , starting from the depth of about 25 cm from the top of the wall and ending below point B, where the resistance of soil in front of the wall is activated, the σ_{res} distribution resembles a trapezium – like in the Rankine’s theory. Yet the values of the resultant stresses there are close to the Rankine’s active pressure only in the case of $\varphi' = \psi' = 42^\circ$. The smaller is the internal angle of friction the smaller is the stress when compared with the Rankine’s active pressure. The highest values of the resultant stress are noted below point B. This is the place where ψ' influence becomes very noticeable (see Fig. 3). In all the cases analysed, if only the surcharge load is greater than 0 kPa, it is observed that

the lower is the ratio α , the greater is the rapid increase of σ_{res} at the bottom of the wall. The biggest observed “jump” equal to 29% (when compared with the stress for $\alpha = 1$) is obtained when $\varphi' = 36^\circ$ and $q = 40$ kPa. Taking into account that the maximum allowable load is not achieved when the difference between ψ' and φ' is lower than 20° [5], the expected increase of stress would probably be even greater for higher values of the surcharge load.

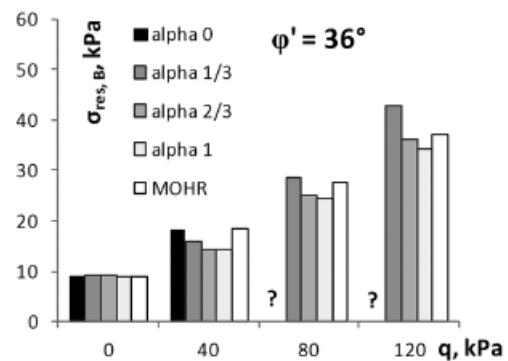


Figure 3. Resultant stresses at point B ($h = 0.5$ m) ($\varphi' = 36^\circ$)

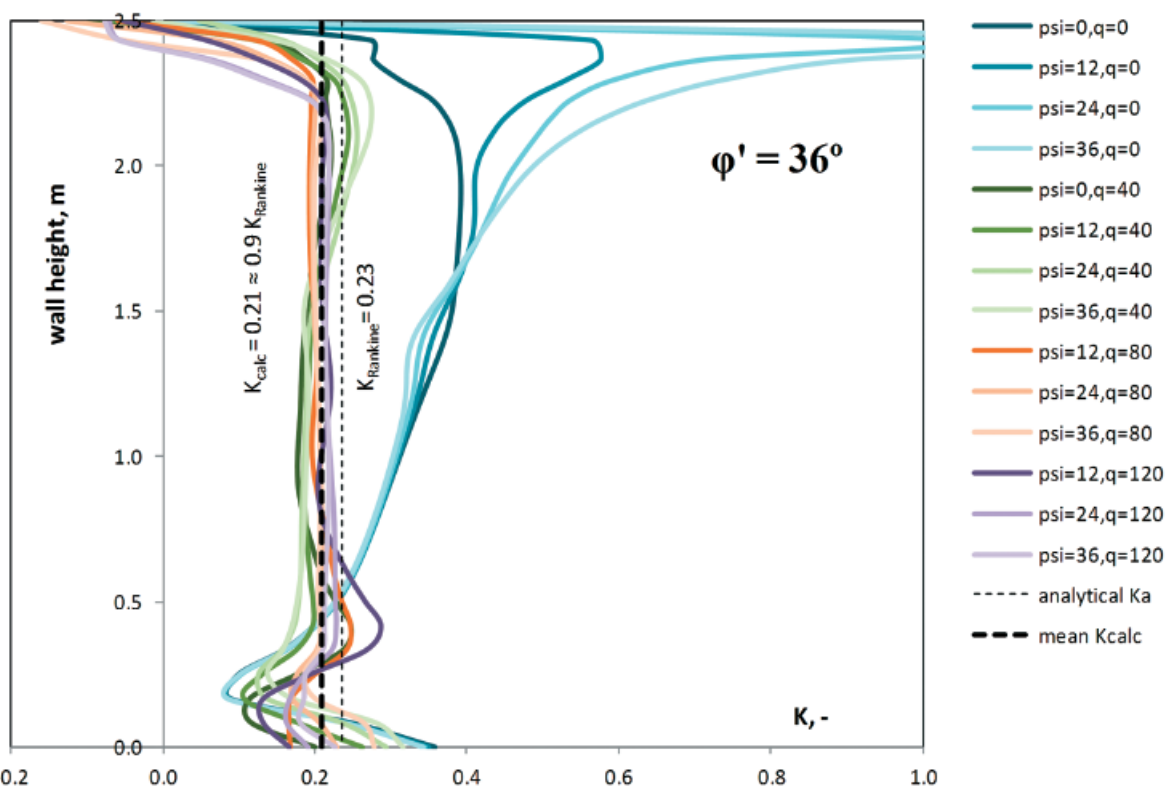


Figure 4. Distribution of K along the segment A-C ($\phi' = 36^\circ$)

Table 2. Values of average K for height: 0.5 m – 2.25 m

ϕ' °	for q = ... kPa	K_{PN} -	K_{num} -	K_{num}/K_{PN} -
30	20 - 60	0.297	0.228	0.8
36	40 - 140	0.235	0.209	0.9
42	80 - 300	0.184	0.187	1.0

The ratio K between the resultant stress acting on the wall σ_{res} and vertical overburden stress ($\gamma'z + q$) (Fig. 1) may be assumed as constant only for the cases where $q \gg 0$ kPa (Fig. 4). The difference between the value of K obtained in the numerical analysis (K_{num}) and the one calculated based on [12] (K_{PN}) according to the Rankine’s proposal for active pressure is decreasing with the increase of ϕ' (Table 2).

The influence of dilatancy angle on K value is clearly visible at the top of the wall, but it concerns only the cases with low surcharge load. This is also true as far as the inclination angle δ is concerned. However, taking into account that the σ_{res} values are small in this region, this impact may be ignored.

4. CONCLUSIONS

Assumption of an associated plastic flow rule ($\psi' = \phi'$) in numerical analyses of retaining walls may result in underestimation of the maximum stress acting in the soil behind the structure. Thus very important becomes estimation of the true dilatancy angle in laboratory or *in situ* tests.

REFERENCES

- [1] *Coulomb C. A.*; Essai sur une application des regles de maximis et minimis a quelques problemes de statique relatifs a l'architecture (The test of the application of the rules of maximum and minimum in some problems of statics in architecture). Mem. de Math. et de Phys., presented at l'Acad. Roy. des Sci., Vol.7, 1776; p.343-387 (in French)
- [2] *Rankine W.J.M.*; On the stability of loose earth. Philosophical Transactions of the Royal Society of London, Vol.147, 1857; p.9-27
- [3] *Potts D. M., Fourie A. B.*; The behaviour of a propped retaining wall: results of a numerical experiment. Geotechnique, Vol.34, No.3, 1984; p.383-404
- [4] *Bowles J. E.*; Foundation analysis and design. Fifth ed., McGraw-Hill, 1997

-
- [5] *Kowalska M.*; Numerical study of the influence of dilatancy angle on bearing capacity and rotation of a gravity retaining wall. Proc. 15. Danube – European Conference on Geotechnical Engineering (DECGE 2014), Vienna, Austria, 2014
- [6] *Serrano A., Olalla C., Perucho A.*; Active and passive earth pressures on retaining walls assuming a non-linear strength criterion and constant dilatancy. Proc. 11. Congress of the International Society for Soil Mechanics, Lisbon, Portugal, 2007
- [7] *Sadrekarimi A., Damavandinejad Monfared S.*; Numerical investigation of the mobilization of active earth pressure on retaining walls. Proc. 18. International Conference on Soil Mechanics and Geotechnical Engineering, Paris, France, 2013
- [8] PN-81/B-03020: Building soils. Foundation bases. Static calculation and design, 1985
- [9] *Yaky J.*; The coefficient of earth pressure at rest. Journal for Society of Hungarian Architects and Engineers, Vol.7, 1944; p.355-358
- [10] *Gryczmański M.*; Jeszcze o przyczynach awarii wysokiego nasypu w km 330+970 autostrady A4 (More about the causes of the damage of high embankment at 330+970 km of the A4 motorway). Proc. 23. Konferencja Naukowo-Techniczna “Awarie Budowlane”, Szczecin – Międzyzdroje, Poland, 2007; p.403-412 (in Polish)
- [11] *Homand-Etienne F., Rapin H., Song Y.*; Effect of aggregates angularity on granular material behaviour. Proc. International Conference on Micromechanics of Granular Media, Powders and Grains, Clermont-Ferrand, France, 1989
- [12] PN-83/B-03010: Retaining walls. Static calculation and design, 1993